

# LEARNING ADJACENCY MATRIX FOR DYNAMIC GRAPH NEURAL NETWORK

Osama Ahmad, Omer Abdul Jalil, Usman Nazir, Murtaza Taj

Computer Vision and Graphics Lab, LUMS

## ABSTRACT

In recent work, [1] introduced the concept of using a Block Adjacency Matrix (BA) for the representation of spatio-temporal data. While their method successfully concatenated adjacency matrices to encapsulate spatio-temporal relationships in a single graph, it formed a disconnected graph. This limitation hampered the ability of Graph Convolutional Networks (GCNs) to perform message passing across nodes belonging to different time steps, as no temporal links were present. To overcome this challenge, we introduce an encoder block specifically designed to learn these missing temporal links. The encoder block processes the BA and predicts connections between previously unconnected subgraphs, resulting in a Spatio-Temporal Block Adjacency Matrix (STBAM). This enriched matrix is then fed into a Graph Neural Network (GNN) to capture the complex spatio-temporal topology of the network. Our evaluations on benchmark datasets, surgVisDom and C2D2, demonstrate that our method, with slightly higher complexity, achieves superior results compared to state-of-the-art results. Our approach's computational overhead remains significantly lower than conventional non-graph-based methodologies for spatio-temporal data.

**Index Terms**— Spatio-Temporal Data, Remote sensing, Superpixels, Learnable Adjacency Matrix

## 1. INTRODUCTION

The arena of spatio-temporal data analysis has rapidly expanded within the domain of deep learning, finding applications in diverse sectors such as traffic management [2], agricultural yield prediction [3], flood risk assessment [4], land cover monitoring [5], ride-sharing demand prediction [6], video-based activity recognition [7], and brain-computer interfaces like EEG-based intention recognition [8]. Spatio-temporal data is inherently complex due to its reliance on both spatial configurations and temporal evolutions [9], necessitating the development of sophisticated models that can handle both these dimensions effectively.

Traditional CNN-based architectures have excelled in spatio-temporal tasks within the Euclidean space, demonstrated by work such as spatial-temporal attention models [10] and 3D-ResNet in change detection for remote sensing [11]. For non-Euclidean structures, Graph Neural Networks (GNNs) have shown promise, particularly when augmented by Recurrent Neural Networks (RNNs) for temporal aspects [12] and modular graph transformers for classification tasks [13, 14, 15].

While significant progress has been made in this domain, existing methods often struggle to holistically model both spatial and temporal information within a unified framework. Most of the existing work allows the evolution of features and connection between vertices [16] however, the addition/deletion of vertices remains a challenging task. A notable attempt to overcome this limitation was the introduction of the Block Adjacency Matrix (BA) [1], which aimed to encapsulate spatio-temporal relationships within a singular

graph. However, the model failed to establish temporal connections between discrete time steps, leading to isolated sub-graphs and consequently limiting the capabilities of Graph Convolutional Networks (GCNs) in message passing.

Our work builds on this foundation by introducing an encoder block to infer the missing temporal connections, thereby constructing an improved adjacency matrix that captures the full spatio-temporal topology. Our key contributions are as follows:

1. A transformer-based encoding architecture that generates a Spatio-Temporal Block Adjacency Matrix (STBAM) thus providing a learnable framework for spatio-temporal graphs.
2. To ensure temporal connections and to avoid any isolated sub-clusters within the graph, we propose a novel loss function that eliminates all but one zero eigen-values from the laplacian of the resulting graph by modulating its sparsity  $\rho$ .
3. We integrate our encoder and loss function into a GNN-based framework, resulting in a novel architecture for representation of spatio-temporal data.
4. We employed our frame-work for spatio-temporal classification in two different domains i.e. Remote Sensing and Action Recognition. The experiments on two benchmark datasets namely C2D2 [11], and surgVisDom [17] show that our method achieved superior performance.
5. Our proposed approach also keeps computational overheads lower than traditional non-graph methods.

## 2. METHODOLOGY

### 2.1. Problem Formulation

A dynamically evolving graph can be defined as a time-ordered sequence  $[\mathcal{G}_1, \mathcal{G}_2, \dots, \mathcal{G}_\tau]$ , where  $\tau$  denotes the total number of time-steps in the sequence. At each time-step  $t$ , the graph  $\mathcal{G}_t$  is characterized by a triple  $(\mathbf{V}_t, \mathbf{A}_t, \mathbf{X}_t)$  as per the survey [18]. These components are described in detail as follows:

1. **Vertices:**  $\mathbf{V}_t$  denotes the set of vertices in the graph at time  $t$ . The cardinality of this set is denoted by  $n_t$ , i.e.,  $|\mathbf{V}_t| = n_t$ .
2. **Adjacency Matrix:**  $\mathbf{A}_t$  is an  $n_t \times n_t$  matrix that describes the connections between the vertices.
3. **Feature Matrix:**  $\mathbf{X}_t$  is an  $n_t \times d$  matrix, where  $d$  represents the dimensionality of the feature space.

Existing methods on dynamic GNNs [19, 20], typically allow varying features and edges over time. However, the addition and removal of nodes is not supported in graph convolution neural networks. In our work, we consider graphs where the number of nodes  $n_t$  and edges can vary over time.

**Problem Definition.** Given a block adjacency matrix BA of the supergraph, the objective is to learn a mapping function  $f$  parameterized by  $\Theta$ . The function  $f$  transforms BA into a new adjacency

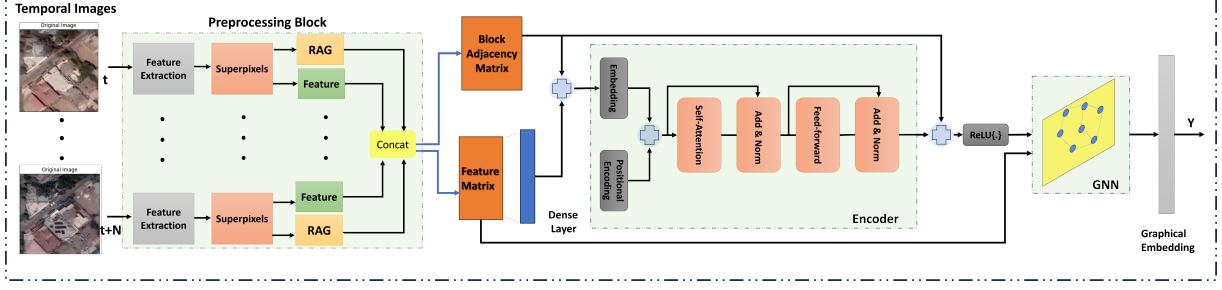


**Fig. 1.** Proposed Framework: STBAM-GNN for Spatio-temporal Analysis consists of 1) Feature Extraction using VGG16, 2) Region Adjacency Graph (RAG) Formation using Superpixels, 3) BA & STBAM and 4) GNN Processing pipeline.

matrix  $BA_M$  such that the graph becomes better connected based on the Laplacian matrix's eigenvalues.

$$BA_M = f(BA; \Theta), \quad (1)$$

s.t.  $\|\lambda_{BA_M}\|_0 > \|\lambda_{BA}\|_0$

Here,  $\|\lambda_{BA_M}\|_0$  and  $\|\lambda_{BA}\|_0$  denote the L0 norm (count of non-zero values in a vector) of the eigenvalues of the Laplacian matrices corresponding to  $BA_M$  and  $BA$ , respectively. The constraint requires that  $BA_M$  has more non-zero eigenvalues than  $BA$ , thereby reducing the number of disconnected components in the graph.

## 2.2. Proposed framework

An overview of the proposed framework is shown in Fig. 1. Although our method is general for spatio-temporal data with varying number of nodes and connection, our focus in this work is on spatio-temporal visual data. Thus our propose methodology has following major components:

1. Generating a supergraph  $BA$  of multiple Region adjacency graphs (RAGs)  $\mathcal{G}^{(i)}$  of superpixels.
2. Encoder architecture for generating modified Spatio-Temporal Block Adjacency Matrix (STBAM) via transformer encoder.
3. Learning STBAM

## 2.3. SuperGraph of RAGs

We first generate a superpixel nodes representation of each image. Then we created a region adjacency graph (RAG) from the superpixel nodes representation by connecting the neighboring nodes. The superpixel are generated using SLIC (Simple Linear Iterative Clustering) algorithm as exemplified in [1] and [21] (see Figure 2). The feature vector of each superpixel is generated using VGG16 [22] trained on ImageNet dataset [23]. To align with the encoder's and GNNs requirement for a desired number of nodes, we perform zero-padding (in case of fewer superpixels) and node dilation (in case of excessive nodes) guided by the output of the SLIC algorithm.

Finally, these region adjacency graph (RAG)  $\mathcal{G}_t$  are combined into a supergraph by concatenating their adjacency matrices diagonally into a block adjacency matrix (BA) represented as:

$$BA = \begin{bmatrix} \mathbf{A}_1 & \mathbf{Z} & \cdots & \mathbf{Z} \\ \mathbf{Z} & \mathbf{A}_2 & \cdots & \mathbf{Z} \\ \vdots & \vdots & \ddots & \vdots \\ \mathbf{Z} & \mathbf{Z} & \cdots & \mathbf{A}_\tau \end{bmatrix}, \quad (2)$$

where  $\mathbf{Z}$  represents matrix of zeros, and  $\mathbf{A}_t$  is the adjacency matrix for  $\mathcal{G}_t$ . Key characteristic properties of this block adjacency matrix

$BA$  are that it is positive semi definite (PSD) and contains N zero eigenvalues for N disconnected subgraphs. The feature representation  $\mathbf{X}$  of the supergraph can be arranged as:

$$\mathbf{X} = [\mathbf{X}_1^T, \mathbf{X}_2^T, \dots, \mathbf{X}_\tau^T]^T, \quad (3)$$

where  $\mathbf{X}_t$  represents the node features of the graph at time-step  $t$ , i.e.,  $\mathcal{G}_t$ . If each node has  $d$  features, the order of  $\mathbf{X}$  will be  $(n\tau \times d)$  where each row will represent the features of a superpixel node.

The supergraph is just a stack of unconnected sub-graphs, each representing the data at 1 time-step. Although this methodology does allow us to use a single GNN for spatio-temporal classification, the GNN is unable to capture the temporal relation between the data at different time-steps because of the temporal data being unconnected. We solve this problem by designing an encoder as discussed next.

## 2.4. Encoder for STBAM

Next, we present the transformation process of the block adjacency matrix ( $BA$ ) as it undergoes encoding within our model. The objective is to create a modified block adjacency matrix ( $BA_M$ ) that captures enhanced temporal relationships between nodes. Our approach, leveraging a Transformer encoder [24], learns the missing temporal links between subgraphs from different time-points, thus allowing the GNN message passing in the temporal dimension.

In our approach a more informative encoding is facilitated by incorporating node features into the sparse adjacency matrix. This is achieved by projecting the node features into a higher-dimensional space using a learnable projection layer  $\mathbf{W}_P$ . This enables the model to discern which features are most relevant when predicting temporal links. The augmented block adjacency matrix ( $\hat{BA}$ ) is formulated as follows:

$$\hat{BA} = BA + (\mathbf{X}\mathbf{W}_P), \quad (4)$$

The core of our approach involves applying a Transformer encoder to  $\hat{BA}$ . A single layer of the encoder consists of multi-head self-attention and position-wise feed-forward networks, and can be expressed as follows:

$$\text{Attention} = \text{softmax} \left( \frac{\mathbf{W}_Q \hat{BA} (\mathbf{W}_K \hat{BA})^T}{\sqrt{d}} \right) \mathbf{W}_V \hat{BA}, \quad (5)$$

$$BA_{\text{norm}} = \text{LayerNorm} \left( \hat{BA} + \text{Attention} \right), \quad (6)$$

$$BA_{\text{ff}} = \text{ReLU} (\mathbf{W}_1 BA_{\text{norm}} + \mathbf{b}_1) \mathbf{W}_2 + \mathbf{b}_2, \quad (7)$$

$$BA_{\text{enc}} = \text{LayerNorm} (BA_{\text{norm}} + BA_{\text{ff}}), \quad (8)$$

The encoder outputs a modified block adjacency matrix  $BA_{\text{enc}}$  which is asymmetric with real values. The matrix is first decomposed into a symmetric matrix by taking the average of the matrix

and its transpose, then a skip connection is added to it to reinforce the spatial edges. The modified adjacency matrix  $\mathbf{BA}_M$  can be described as:

$$\mathbf{BA}_M = \text{ReLU}(\mathbf{BA} + \frac{\mathbf{BA}_{\text{enc}} + \mathbf{BA}_{\text{enc}}^T}{2}), \quad (9)$$

The ReLU makes sure that there are no negative edge weights. During inference, the edges are thresholded to  $\{0, 1\}$ .

## 2.5. Learning Encoder

**Loss function:** Our encoder and GNN are co-trained for spatio-temporal classification using a novel loss function,  $\mathcal{L}$ , which combines cross-entropy and a sparsity-promoting term:

$$\mathcal{L} = - \sum_{i=1}^N y_i \log(\hat{y}_i) + \lambda \left\| \frac{\mathbf{BA}_{\text{enc}} + \mathbf{BA}_{\text{enc}}^T}{2} \right\|_p. \quad (10)$$

The sparsity term uses the element-wise L1 norm to encourage a sparse block adjacency matrix. Training involves the following condensed steps:

1. Compute node representations  $\mathbf{z} = \text{GNN}(\mathbf{BA}_M, \mathbf{X})$ .
2. Concatenate into  $\mathbf{z}_{\text{concat}} = \text{Concat}(\mathbf{z}_1, \dots, \mathbf{z}_N)$ .
3. Calculate  $\mathbf{h} = \mathbf{W}_G^T \mathbf{z}_{\text{concat}} + \mathbf{b}_G$ .
4. Obtain output  $\mathbf{y} = \text{softmax}(\mathbf{h})$ .

In our approach, we utilize the Graph Attention Network (GAT) as a component to perform feature transformation and attention-based aggregation [25]. Briefly, the core equations of GAT for layer  $l$  can be summarized as follows:

$$\mathbf{h}_i^{(l)} = \mathbf{W}^{(l)} \mathbf{h}_i^{(l-1)}, \quad (11)$$

$$e_{ij}^{(l)} = \text{LeakyReLU} \left( \mathbf{a}^{(l)T} (\mathbf{h}_i^{(l)} \parallel \mathbf{h}_j^{(l)}) \right), \quad (12)$$

$$\alpha_{ij}^{(l)} = \frac{\exp(e_{ij}^{(l)})}{\sum_{k \in \mathcal{N}(i)} \exp(e_{ik}^{(l)})}, \quad (13)$$

$$\mathbf{h}_i^{(l+1)} = \sigma \left( \sum_{j \in \mathcal{N}(i)} \alpha_{ij}^{(l)} \mathbf{h}_j^{(l)} \right), \quad (14)$$

Here,  $\mathbf{W}^{(l)}$  is the weight matrix for linear transformation,  $\mathbf{a}^{(l)}$  is the attention mechanism parameter,  $\alpha_{ij}^{(l)}$  is the normalized attention coefficient, and  $\sigma$  is an activation function.

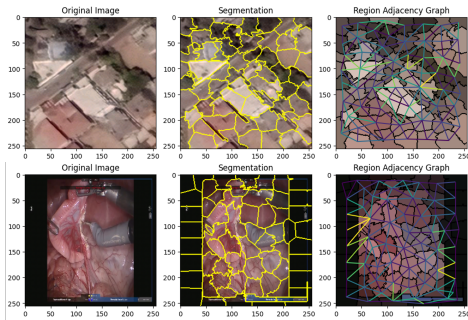


**Fig. 2.** SuperPixel representation on image obtained via SLIC (Row 1) Satellite data. (Row 2) Surgical data.

## 3. RESULTS

### 3.1. Datasets and Implementation Details

We perform experiments on two different datasets.

**SurgVisDom dataset:** Surgical Visual Domain Adaptation dataset [17] consists of three class classification tasks: needle-driving (ND), dissection (DS), and knot-tying (KT). The training data consists of 476 total videos, 450 clips from virtual reality, and 26 clips from real-time clinical data. The testing data consists of 16 clips from clinical data. For training we divide each training sample into 16 equal segments and take 1 random frame from each segment, this gives us 16 frames from each sample. We also over sample every video to increase our training data. We employ a dilated sliding window scheme for frame-by-frame predictions.

**C2D2 dataset:** Its a remote sensing-based dataset consisting of four classes construction, destruction, cultivation, and decultivation [11]. It contains the temporal samples of the years 2011, 2013, and 2017 from Digital Globe. It visits almost 5,50,000 random locations which make approximately  $5310 \text{ km}^2$ . Where they cropped images of  $256 \times 256$  at zoom level 20 which corresponds to 0.149 pixel per meter on the equator.

**Implementation Details:** Experiments are conducted on a Linux machine equipped with an Intel(R) i9 12<sup>th</sup> Gen @ 2.40 GHz, 32 GB RAM, and NVIDIA 3080Ti GPU. The proposed method was implemented using PyTorch, specifically torch geometric for graph operations. Each model was trained using Adam optimizer with an initial learning rate of  $1e^{-3}$  for 200 epochs and a patience of 20, the model with the best accuracy on the validation set was used.

### 3.2. Ablation study

We performed ablative study by comparing 6 different variants of our method. These variants are generated by changing number of superpixel/image, penalty term for sparsity, and norm. To measure the achieved sparsity  $\rho$ , we define, for any sparse matrix  $\mathbf{S}$  with dimensions  $m \times n$ ,

$$\rho(\mathbf{S}) = \frac{m \times n - \text{count}(\mathbf{S} \neq 0)}{m \times n}, \quad (15)$$

where,  $\text{count}(\mathbf{S} \neq 0)$  counts the number of non-zero elements in  $\mathbf{S}$ . The difference in sparsity between  $\mathbf{BA}$  and  $\mathbf{BA}_M$  is defined as

$$\Delta\rho = \frac{\sum_N \rho(\mathbf{BA}) - \sum_N \rho(\mathbf{BA}_M)}{N}, \quad (16)$$

where the sum over  $N$ , refers to averaging over the entire test dataset. It can be seen from Table 1 that our best performing architecture is with 64 superpixels/image using  $L1$  norm and a penalty  $\lambda$  of  $1e^{-5}$ . We used this variant of our architecture for comparison with state-of-the-art methods as discussed next.

### 3.3. Comparative Analysis

We performed comparison with two state-of-the-art algorithms namely 3D-ResNet-34 [11] and STAG-NN-BA-GSP [1] on C2D2 dataset (Table 2) and two state-of-the-art algorithms by team SK [17] and team Parakeet [17] on SurgVisdom dataset (Table 3). It can be seen from Table 2 that our proposed STBAM-64 model achieved highest accuracy of 80.67% on C2D2 dataset which having significantly less parameters as compared 3D-ResNet-34. The slight increase in parameters as compared to STAG-NN-BA-GSP is due to the encoder block in our architecture for generating modified adjacency matrix.

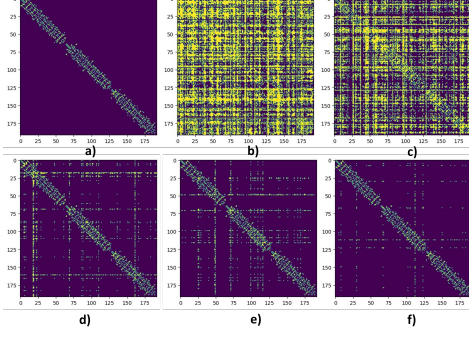


**Fig. 3.** Block adjacency matrix visualization (a) original block adjacency (b) modified with no norm (c) modified with L2 norm,  $\lambda = 1e - 6$  (d) modified with L1 norm,  $\lambda = 1e - 7$  (e) modified with L1 norm,  $\lambda = 1e - 6$  (f) modified with L1 norm,  $\lambda = 1e - 5$ .

**Table 1.** Ablative study on C2D2 Dataset.

Method	Penalty	Sparsity $\rho$ ( $\Delta\rho$ )	Norm	#Param.	Acc. (%)
STBAM-64	$1e^{-7}$	0.9396 (0.0347)	L1	3.392	80.33%
STBAM-64	$1e^{-6}$	0.9467 (0.0276)	L1	3.392	<b>80.67%</b>
STBAM-64	$1e^{-5}$	0.9650 (0.0093)	L1	3.392	80.33%
STBAM-64	0	0.4779 (0.4964)	No	3.392	75.00%
STBAM-64	$1e^{-6}$	0.6436 (0.3307)	L2	3.392	77.33%
STBAM-100	$1e^{-6}$	0.0042 (0.9801)	L1	3.524	75.00%

Similarly, on SurgVisdom dataset, it can be seen from Table 3 that our method achieved highest F1-score and comparable global F1-score and balanced accuracy. In this dataset the training was performed on synthetic data and testing was done on real data to evaluate the problem of domain adaptation. Despite of the fact that, as compared to other methods, we did not introduce any additional steps to solve the domain adaptation problem, our method showed better or comparable results. This illustrated the generalization capabilities of our proposed method.

These results indicates that by addressing the inherent limitations of the block adjacency matrix, which traditionally focuses solely on spatial connections, our encoder block provides a more holistic view of network dynamics by ensuring the graph’s connectivity across different time steps, enriching the data representation for more accurate and comprehensive analysis.

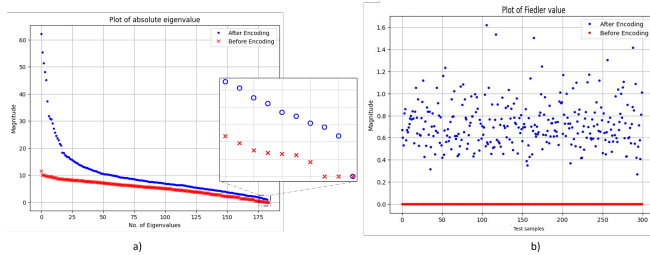


**Fig. 4.** (a) Absolute eigenvalues of Laplacian matrix before & after encoding (b) Fiedler values on the test set before & after encoding.

**Table 2.** Comparative evaluation on C2D2 dataset.

Method	#Param(M)	Accuracy
3D-ResNet-34 [11]	63.50	57.72%
STAG-NN-BA-GSP [1]	0.030	77.83%
STBAM-64 (ours)	3.392	<b>80.67%</b>

**Table 3.** Comparative evaluation on SurgVisdom dataset (hard domain adaptation)

Method	Weighted F1-score	Global F1-score	Balanced Accuracy
Rand [17]	0.45	0.327	0.327%
SK [17]	0.46	0.370	0.369%
Parakeet [17]	0.47	<b>0.475</b>	<b>0.559%</b>
STBAM-64 (ours)	<b>0.53</b>	0.40	0.447%

### 3.4. Eigenvalue and Fiedler Value Analysis

The number of zero eigenvalues in the Laplacian matrix can be insightful regarding graph connectivity, in Fig. 3.3(a) we plot the eigenvalues of the block adjacency matrix before and after encoding for a sample from C2D2 dataset. Specifically, N zero eigenvalues indicate the presence of N unconnected sub-graphs. In our original matrix, we observe 3 zero eigenvalues, corresponding to 3 time steps of data, suggesting a fragmented graph. In contrast, our modified matrix exhibits only 1 zero eigenvalues, indicating improved graph connectivity, which aligns with the successful integration of temporal information by the encoder block.

Figure 3.3(b) illustrates the Fiedler values (also known as the Algebraic Connectivity of the graph) of the block adjacency matrix before and after the encoding block for the entire test set of the C2D2 dataset. The Fiedler value, which is the second smallest eigenvalue of the Laplacian matrix, serves as an indicator of a graph’s connectivity [26]. A Fiedler value of zero generally suggests that the graph is disconnected or poorly connected. In our analysis, the Fiedler values of the original block adjacency matrix are all zero, underlining the presence of disconnected sub-graphs. On the other hand, the modified block adjacency matrices show, on average, much higher Fiedler values. This indicates that our proposed model not only addresses the issue of unconnected sub-graphs but also enhances the overall graph connectivity, thereby facilitating more effective message passing in the temporal dimension.

## 4. CONCLUSION

This work introduces a significant contribution by extending graph convolution message-passing to incorporate temporal dimensions. Traditional models, constrained by the block adjacency matrix, limit message-passing to spatial nodes, hindering the capture of dynamic changes over time. The newly introduced encoder block effectively bridges this gap, enabling a more nuanced understanding of spatio-temporal phenomena and enhancing predictive capabilities.

Future directions include optimizing the encoder block for scalability in handling large-scale graphs with numerous nodes. This may involve algorithmic enhancements and hardware acceleration to address real-time processing and memory constraints. Additionally, the encoder block’s utility for predicting temporal links in evolving graphs holds promise in domains like social network analysis, traffic management, and bioinformatics, offering robustness and performance on larger datasets.



## 5. REFERENCES

- [1] U. Nazir, W. Islam, and M. Taj, "Spatio-temporal driven attention graph neural network with block adjacency matrix (stag-nn-ba)," *arXiv:2303.14322*, 2023.
- [2] Bing Yu, Haoteng Yin, and Zhanxing Zhu, "Spatio-temporal graph convolutional networks: A deep learning framework for traffic forecasting," *arXiv preprint arXiv:1709.04875*, 2017.
- [3] P. Bose, N. K. Kasabov, L. Bruzzone, and R. N. Hartono, "Spiking neural networks for crop yield estimation based on spatiotemporal analysis of image time series," in *IEEE Transactions on Geoscience and Remote Sensing*, vol. 54, no. 11, pp. 6563–6573, 2016.
- [4] Yukai Ding, Yuelong Zhu, Jun Feng, Pengcheng Zhang, and Zirun Cheng, "Interpretable spatio-temporal attention lstm model for flood forecasting," *Neurocomputing*, vol. 403, pp. 348–359, 2020.
- [5] Ava Vali, Sara Comai, and Matteo Matteucci, "Deep learning for land use and land cover classification based on hyperspectral and multispectral earth observation data: A review," *Remote Sensing*, vol. 12, no. 15, pp. 2495, 2020.
- [6] Xu Geng et al., "Spatiotemporal multi-graph convolution network for ride-hailing demand forecasting," in *Proceedings of the AAAI conference on artificial intelligence*, vol. 33, no. 1, pp. 3656–3663, 2019.
- [7] D. Wu, N. Sharma, and M. Blumenstein, "Recent advances in video-based human action recognition using deep learning: A review," *International Joint Conference on Neural Networks (IJCNN)*, pp. 2865–2872, 2017.
- [8] D. Zhang, L. Yao, K. Chen, X. Chang S. Wang, and Y. Liu, "Making sense of spatio-temporal preserving representations for eeg-based human intention recognition," in *IEEE Transactions on Cybernetics*, vol. 50, no. 7, pp. 3033–3044, 2020.
- [9] S. Wang, J. Cao, and P. S. Yu, "Deep learning for spatio-temporal data mining: A survey," in *IEEE Transactions on Knowledge and Data Engineering*, vol. 34, no. 8, pp. 3681–3700, 2022.
- [10] Chen Hao and Zhenwei Shil, "A spatial-temporal attention-based method and a new dataset for remote sensing image change detection," *Remote Sensing*, vol. 12, 2020.
- [11] Muhammad Ahmed Bhimra, Usman Nazir, and Murtaza Taj, "Using 3d residual network for spatio-temporal analysis of remote sensing data," *ICASSP*, pp. 1403–1407, 2019.
- [12] Isaiah J. King and H. Howie Huang, "Euler: Detecting network lateral movement via scalable temporal link prediction," *ACM Transactions on Privacy and Security*, 2023.
- [13] Nguyen HD, Vu XS, and Le DT, "Modular graph transformer networks for multi-label image classification," in *Proceedings of the AAAI conference on artificial intelligence*, vol. 35, no. 10, pp. 9092–9100, 2021.
- [14] Cunjun Yu et al., "Spatio-temporal graph transformer networks for pedestrian trajectory prediction," *ECCV, Glasgow, UK, August 23–28, 2020, Proceedings*, pp. 507–523, 2020.
- [15] S. Yun, M. Jeong, R. Kim, J. Kang, and H. J. Kim, "Graph transformer networks," *Advances in neural information processing systems*, 2019.
- [16] Guangyin Jin, Yuxuan Liang, Yuchen Fang, Jincui Huang, Junbo Zhang, and Yu Zheng, "Spatio-temporal graph neural networks for predictive learning in urban computing: A survey," 2023.
- [17] Zia A et al., "Surgical visual domain adaptation: Results from the miccai 2020 surgvisdom challenge," *arXiv preprint arXiv:2102.13644*, 2021.
- [18] Zonghan Wu et al., "A comprehensive survey on graph neural networks," *IEEE Transactions on Neural Networks and Learning Systems*, vol. 32, no. 1, pp. 4–24, 2021.
- [19] Meng Jiang, Taeho Jung, and et al., "Federated dynamic graph neural networks with secure aggregation for video-based distributed surveillance," *ACM Transactions on Intelligent Systems and Technology*, vol. 13, no. 4, pp. 1–23, 2022.
- [20] Pareja A, Domeniconi G, Chen J, Ma T, Suzumura T, Kanezashi H, Kaler T, Schardl T, and Leiserson C, "Evolvegcn: Evolving graph convolutional networks for dynamic graphs," in *Proceedings of the AAAI conference on artificial intelligence*, pp. 5363–5370, 2020.
- [21] A. M. Censi et al., "Attentive spatial temporal graph cnn for land cover mapping from multi-temporal remote sensing data," *IEEE Access*, vol. 9, pp. 23070 – 23082, 2021.
- [22] K. Simonyan and A. Zisserman, "Very deep convolutional networks for large-scale image recognition," *arXiv:1409.1556*, 2014.
- [23] J. Deng, W. Dong, R. Socher, L. J. Li, Kai Li, and Li Fei-Fei, "Imagenet: A large-scale hierarchical image database," *IEEE Conference on Computer Vision and Pattern Recognition*, pp. 248–255, 2009.
- [24] A. Vaswani et al., "Attention is all you need," *Advances in neural information processing systems*, 2017.
- [25] Velickovic, Petar, Guillem Cucurull, Arantxa Casanova, Adriana Romero, Pietro Lio, and Yoshua Bengio, "Graph attention networks," *ICLR*, 2018.
- [26] Miroslav Fiedler, "Algebraic connectivity of graphs," *Czechoslovak Mathematical Journal*, vol. 23, no. 2, pp. 298–305, 1973.